Proceedings of ICRC 2001: 2810 © Copernicus Gesellschaft 2001

ICRC 2001

The Status of the STACEE Observatory

C. E. Covault[1], L. M. Boone[2], D. Bramel[3], E. Chae[4], P. Fortin[5], D.M Gingrich[6,7], J. A. Hinton[4], D. S. Hanna[5], R. Mukherjee[3], C. Mueller[5], R.A. Ong[8], K. Ragan[5], R. A. Scalzo[4], D. R. Schuette[8], C. G. Theoret[5], and D. A. Williams[2]

[1]Department of Physics, Case Western Reserve University, Cleveland, OH 44106, USA
[2]Santa Cruz institute for Particle Physics, University of California, Santa Cruz, CA 95064, USA
[3]Columbia University & Barnard College, New York, NY 10027, USA
[4]Enrico Fermi Institute, University of Chicago, 5640 Ellis Av., Chicago, IL 60637, USA
[5]Department of Physics, McGill University, Montreal, Quebec H3A 2T8, Canada
[6]Centre for Subatomic Research, University of Alberta, Edmonton, Alberta T6G 2N5, Canada
[7]TRIUMF, Vancouver, British Columbia V6T 2A3, Canada
[8]Department of Physics & Astronomy, University of California, Los Angeles, CA 90095, USA

Abstract. The Solar Tower Atmospheric Cherenkov Effect Experiment (STACEE) is a ground-based instrument designed to study astrophysical sources of gamma radiation in the energy range of 50 to 500 GeV. STACEE uses an array of large heliostat mirrors at the National Solar Thermal Test Facility in Albuquerque, New Mexico, USA. The heliostats are used to collect Cherenkov light produced in γ-ray air showers. The light is concentrated onto an array of photomultiplier tubes located near the top of a tower. The construction of STACEE started in 1997 and has been completed in 2001. During the 1998-99 observing season, we used a portion of the experiment, STACEE-32, to detect γ-rays from the Crab Nebula. The completed version of STACEE uses 64 heliostat mirrors, having a total collection area of 2300 m^2. During the last year, we have also installed custom electronics for pulse delay and triggering, and 1 GHz Flash ADCs to read out the photomultiplier tubes. The commissioning of the full STACEE instrument is underway. Preliminary observations and simulation work indicate that STACEE will have an energy threshold below 70 GeV and a reach for extragalactic γ-ray sources out to redshift of $\sim$1.0. In this paper we describe the design and performance of STACEE.

1 Overview

STACEE (The Solar Tower Atmospheric Effect Experiment) is a new experiment constructed for ground-based gamma-ray astrophysics. STACEE detects γ-rays via the atmospheric Cherenkov radiation produced in extensive air showers. STACEE uses 64 large solar mirrors (heliostats) as the primary collector of Cherenkov photons. This very large collection area allows STACEE to probe a region of γ-ray energies (50-500 GeV) not yet explored by previous imaging Cherenkov instruments.

STACEE is located at the National Solar Thermal Test Facility (NSTTF) at Sandia National Laboratories in Albuquerque, New Mexico, USA (see Figure 1). STACEE is one of four solar-tower Cherenkov experiments that are currently in operation or under development. These include the French CELESTE experiment in the Pyrenees (La Gallou, 2001) the Spanish/German GRAAL experiment (Arqueros, 1999) and the Solar Two Gamma-Ray Observatory near Barstow, California (Zweerink, 1999).

Correspondence to: C. E. Covault
(covault@hep.uchicago.edu)

Fig. 1. Aerial view of National Solar Tower Test Facility at Sandia National Laboratories in Albuquerque, New Mexico, USA.

The STACEE experiment has been built in stages, with each stage using progressively more heliostats and progressively improved optics and electronics all of which are incorporated in the final STACEE experiment that is now complete. Figure 2 shows a plan view of the heliostats at the NSTTF used for each stage of the STACEE experiment. The stages of construction are delineated as follows:

. **STACEE-32:** Construction on STACEE began in 1997. By October of 1998 we commissioned a partially complete system with two secondary mirrors and 32 heliostats called STACEE-32. Dur-

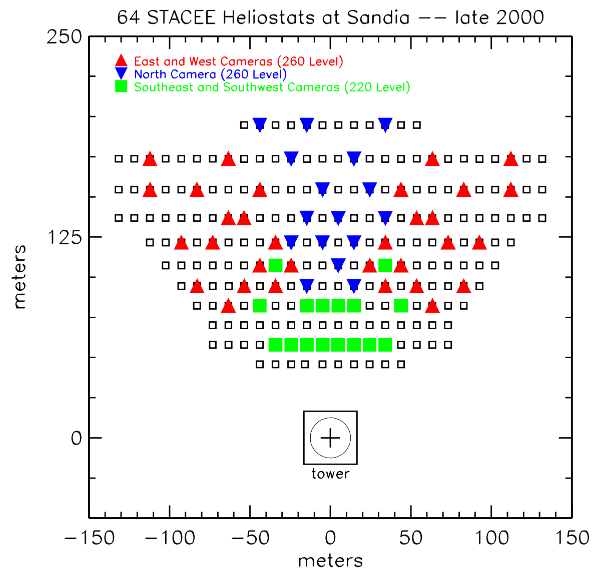

Fig. 2. Plan view of NSTTF showing heliostats used for STACEE. STACEE-32 used the East and West Cameras; STACEE-48 used the East, West, and North Cameras.

ing the 1998-1999 observing seasons, we operated STACEE-32 to measure instrument performance and to conduct initial observations of gamma-ray sources. These results have been reported elsewhere (Ong, 2000; Covault, 2000). In particular, we observed the Crab nebula and pulsar between December 1998 and March 1999 with STACEE-32. We detected the Crab with high statistical significance (seven standard deviations) at an energy of threshold of 190 $\pm$ 60 GeV. This detection represents the first astrophysical results from STACEE (Oser, 2001) and demonstrated the viability of the instrument concept.

. **STACEE-48:** A second stage of the partially completed STACEE instrument was constructed during 1999 and 2000, with 48 heliostat channels active. In addition, several key improvements were made to the optics and electronics (see below). STACEE-48 has been operating as a gamma-ray observatory since November 2000. Sources observed thus far with STACEE-48 include Markarian 421, which has been detected by STACEE with high significance (Hinton, 2001), and Markarian 501 (Ong, 2001).

. **STACEE:** Construction of the full STACEE instrument with 64 heliostat channels and five secondary mirrors is now complete. Regular operation of the completed STACEE experiment as a gamma-ray observatory is expected to commence by Fall, 2001. At this point STACEE will operate continuously for several years (Ong, 2001).

2 Completion of the STACEE instrument

During the last two years, we have worked on the completion of the STACEE instrument. We carried out the following tasks:

– We have learned that the alignment of the heliostat facets is an important consideration for the overall optical throughput. To obtain the best throughput possible, we have developed a precise algorithm for setting facet headings using lasers and a telescope. Individual facet headings are now determined with an accuracy corresponding to $\lesssim$20 cm of movement of the heliostat spot at the position of the secondary mirror.

– A set of alignment lasers has been mounted at key positions on the optical structures on the tower to verify and monitor the optical alignment of secondary mirrors and cameras. Individual PMT positions are now verified monthly using a CCD camera and moonlight. We have also used moonlight to directly determine the proper bias (offset) heading for each heliostat to obtain maximum light throughput.

– To reduce background light due to reflected albedo, the asphalt field beneath the heliostats was coated by a dark black sealant. This coating reduced the albedo by up to 50%.

– An infrared cloud monitor and an optical photometer (which tracks a star close to the STACEE field of view) are being commissioned to work along with STACEE.

During the last two years, we have also made a push to install the final STACEE electronics. This work included the installation and integration of additional trigger electronics to support all 64 PMT channels. We have designed and installed a custom dynamic delay and trigger system, based in VME using FPGA technology (Martin and Ragan, 2000). The system features delays programmable in 1-nsec steps over a one-microsecond range and a two-level multiplicity trigger with an adjustable trigger coincidence gate (currently set at 12 nsec). The trigger system keeps a record of hits on each channel for the 32 nsec window surrounding a trigger, with a 1 nsec accuracy.

We have also completed the installation of high speed (1 GHz) 8-bit FADCs to digitize signals from the PMT channels. These state-of-the-art digitizers (Acqiris DC270) provide the accurate time and amplitude measurements necessary for complete shower reconstruction. Improved shower reconstruction will help STACEE achieve a better angular resolution and gamma/hadron separation (and hence sensitivity).

Figure 3 shows a schematic of the electronics for STACEE. The FADCs measure the analog pulse of each PMT channel to determine its time-of-arrival and amplitude. They also measure the instantaneous night sky background before and after the Cherenkov signals. The FADCs serve as an analog pipeline to buffer the PMT information while the trigger decision is being made. Conventional multi-hit TDCs are used for verification of the pulse timing.

The FADCs used by STACEE are packaged in a 4-channel compact-PCI (cPCI) board, and are controlled using a real-time Linux-based DAQ that operates in conjunction with

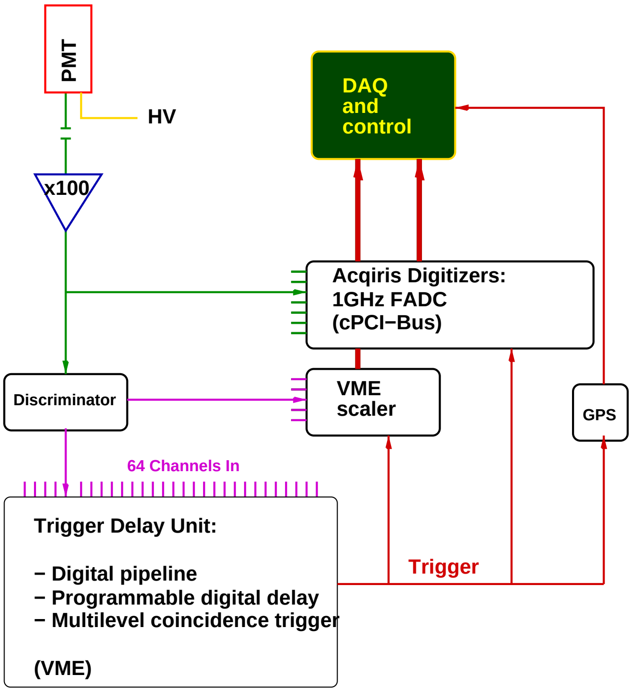

Fig. 3. Schematic of STACEE electronics, including the new delay/trigger circuitry and the Acqiris digitizers.

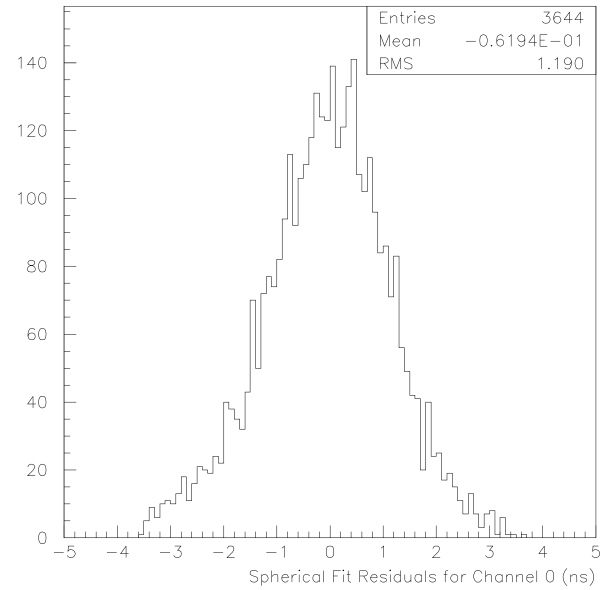

Fig. 4. Timing residuals on a single STACEE channel relative to best-fit spherical wavefront reconstruction. The RMS of this distribution is 1.2 ns, indicating that STACEE is achieving excellent time resolution.

the VME-based trigger system. STACEE personnel developed and implemented the entire suite of software required for the DAQ, including the kernel-based device driver; this work was necessary because the base drivers written for Windows NT would have unacceptable dead-time. A full crate of FADCs to provide readout for 48 PMT channels has been installed, and the commissioning tests indicate that we will be able to readout the FADCs with a very small dead-time ($\sim$2 ms/event, as compared to $\sim$10 ms/event for the VME portion of the DAQ). The raw data taken by the FADCs is fully integrated into the standard STACEE analysis chain, and during the summer we will finalize the reconstruction algorithms to provide robust estimates of the pulse amplitude and time.

3 Recent performance results from STACEE-48

A concerted effort is underway to characterize the detector performance. These studies are based upon *in situ* calibration, Monte Carlo simulation, and the analysis of data taken. Event reconstruction parameters, in particular, angular reconstruction and energy determination, are primarily determined from the arrival times and pulse amplitudes of the Cherenkov signal seen at each heliostat. Thus, calibrating and characterizing STACEE's timing resolution and optical response is critical. Here we present some of the results that have been obtained thus far in this effort.

We have developed an initial reconstruction scheme that is applied to the STACEE Cherenkov data. To reconstruct the arrival direction of an incoming shower, the times recorded by the TDCs (after calibration and trims are applied) are fit to a spherical shape. Figure 4 shows a plot of the timing residuals on one channel after best fit spherical wavefront reconstruction. The residual width of $\sim$1 ns is at the level predicted by simulation indicating that the timing measurement from any one channel is primarily limited by the intrinsic fluctuations in the shower.

We obtain an estimate of the pointing accuracy of STACEE by dividing the array into two overlapping sub-arrays and using each sub-array to reconstruct the arrival direction separately. The angular difference between the reconstructed directions from the sub-arrays, as shown in Figure 5, is a measure of the intrinsic angular resolution (modulo a statistical correction factor). From this study we determine an angular resolution of $\lesssim 0.2^o$, which agrees with simulation and the design value. Figure 5 also shows the reduced χ^2 distribution for the goodness-of-fit to a spherical wavefront.

Another key indicator of detector performance is the trigger rate versus discriminator threshold curve which provides a good measure of the effective operating threshold of the experiment. Figure 6 shows this curve for STACEE-48 observing cosmic rays coming from the zenith. Using this data, we can set the operating threshold at the lowest possible value that ensures a negligible contribution to the rate from accidental triggers on night-sky noise. We note that for STACEE-48, the usable threshold is constrained by the intrinsic limit of 16 hits per channel on multi-hit TDCs and by deadtime associated with individual discriminators. The recent installation of FADCs will allow us to run STACEE at the lowest possible trigger threshold, which translates into the lowest possible energy threshold.

Finally, work is in progress to compare in detail results from simulations against data collected by the experiment to

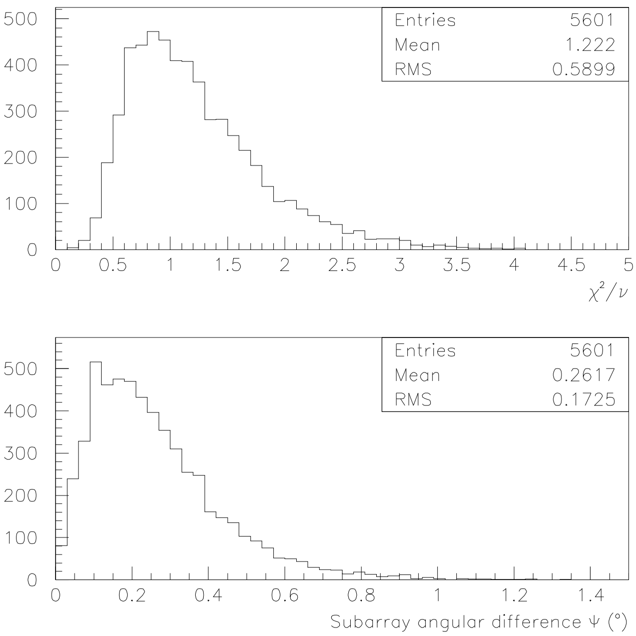

Fig. 5. Top: Distribution of reduced χ^2 values from the best fit spherical wave front to arrival times recorded at each heliostat. **Bottom** Split-array reconstructed direction difference, which is a good estimate of angular position resolution on reconstructed showers.

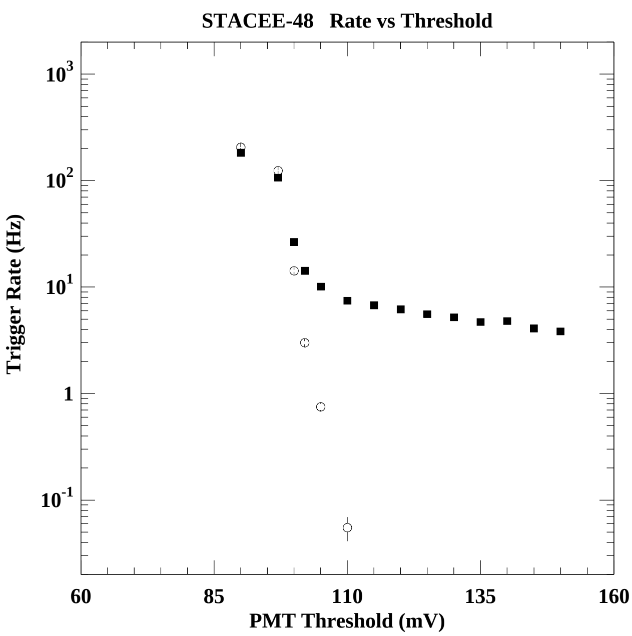

Fig. 6. Trigger rate versus discriminator threshold for STACEE-48. The black squares indicate the response of the experiment with channel delays set in-time for Cherenkov triggers. The open circles, taken with delays times scrambled, represent the rate due to accidental triggers on the night sky background. The turnover at rates above 100 Hz is due to DAQ deadtime. Above a threshold of 120 mV, the experiment operates with Cherenkov rate $\gtrsim$7.5 Hz and with negligible accidental background. For comparison, one photo-electron corresponds to $\sim$25 mV.

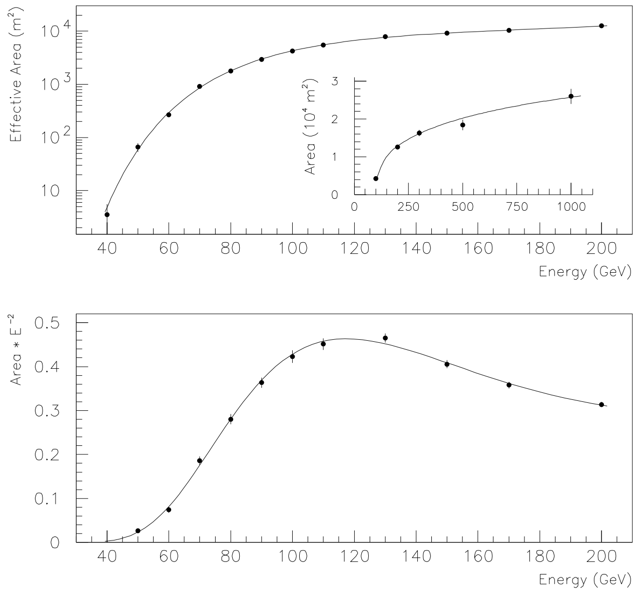

Fig. 7. The STACEE-48 energy response to γ-rays based on Monte Carlo simulations. Our preliminary estimate of the energy threshold is 120 ± 25 GeV at zenith for observations made in Winter/Spring 2001. This energy threshold is appropriate for observations made with a 145 mV PMT threshold, well above the threshold where the rate of accidental triggers becomes neglibible.

determine energy threshold. We use the CORSIKA package to simulate air showers (Heck, 1998). Figure 7 shows the preliminary energy response of the STACEE-48 system to simulated γ-rays for data taken Winter/Spring 2001 giving a threshold of 120 ± 25 GeV assuming a source spectrum of the form E^{-2} located at zenith. With the implementation of FADCs for STACEE we expect to operate at a lower threshold ($\lesssim$100 GeV).

Acknowledgements. We are grateful to the staff at the NSTTF for their excellent support. Thanks to Gora Mohanty, Jeff Zweerink, Tumay Tumer, Marta Lewandowska, Scott Oser, and François Vincent. This work was supported in part by the National Science Foundation (under Grant Numbers PHY-9983836, PHY-0070927, and PHY-007095), the Natural Sciences and Engineering Research Council, FCAR (Fonds pour la Formation de Chercheurs et l'Aide à la Recherche), the Research Corporation, and the California Space Institute. CEC is a Cottrell Scholar of Research Corporation.

References

Arqueros, F., et al., *Proc. 26th ICRC, Salt Lake City*, **5**, 215, 1999.
Covault, C.E. et al., *Towards a Major Atmospheric Cherenkov Detector VI: (Snowbird, UT) conf. proc.* AIP Press, 411–415, 2000.
Heck, D. et. al., FZKA 6019, Forschungzentrum Karlsruhe, 1998.
Hinton, J.A., et al., These Proceedings.
Martin, J.-P. and Ragan, K., *Proc. IEEE Nuclear Science Symposium, Lyon, France*, 2000.
Ong, R.A., et al., *Towards a Major Atmospheric Cherenkov Detector VI: (Snowbird, UT)* AIP Press, 401–410, 2000.
Ong, R.A., et al., These Proceedings.
Oser, S. et al., ApJ., 547, 949–958, 2001.
La Gallou, R. et al., These Proceedings.
Zweerink, J.A. et al., *Proc. 26th ICRC, Salt Lake City*, **5**, 223, 1999.